

# Copolymerization of alpha-methyl styrene with butyl acrylate in bulk

N.T. McManus<sup>a</sup>, A. Penlidis<sup>a,\*</sup>, M.A. Dube<sup>b</sup>

<sup>a</sup>Department of Chemical Engineering, University of Waterloo, Waterloo, Ont., Canada N2L 3G1

<sup>b</sup>Department of Chemical Engineering, University of Ottawa, Ottawa, Ont., Canada K1N 6N5

Received 30 July 2001; received in revised form 23 October 2001; accepted 25 October 2001

## Abstract

The kinetics of the copolymerization of alpha-methyl styrene (AMS) and butyl acrylate (BA) have been studied for the first time. Reactivity ratios for the system have been assessed over a range of temperatures (60–140 °C). Copolymerization models that account for monomer depropagation have been considered in order to determine the importance of depropagation effects for the chosen set of reaction conditions. Full conversion range experiments have been carried out to assess the effects of feed composition, temperature and initiator concentration on polymerization kinetics. © 2002 Elsevier Science Ltd. All rights reserved.

**Keywords:** Alpha-methyl styrene; Butyl acrylate; Reactivity ratios

## 1. Introduction

Multicomponent polymers based on styrene/acrylate formulations are a basis for many important applications such as paints and coatings. This has stimulated the considerable body of study on copolymerizations of styrene with various acrylate monomers [1]. The practical interest in copolymers of AMS and acrylate monomers stems in part from the fact that AMS extends the useful temperature range of the copolymers as a result of the high value of the glass transition temperature ( $T_g$ ) for poly-AMS (ca. 170 °C).

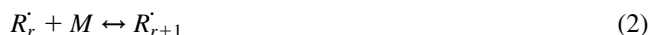
Free radical polymerization of AMS is highlighted by difficulties in producing high molecular weight polymer at reasonably fast rates of reaction. Polymerizations in the normal temperature range (40–90 °C) are slow in bulk and solution. This is in part due to the fact that the monomer exhibits a relatively low  $k_p/k_t$  ratio [2]. Attempts to circumvent this have used emulsion polymerization as one means of obtaining higher rates by offsetting rate reductions caused by the relatively high termination rates [3].

The current work was stimulated by another obvious method to offset slow reaction rates with the use of elevated reaction temperatures. In order to model and to make useful predictions about the behavior of AMS in copolymerizations at such reaction conditions, there is a need to expand the current body of experimental data. In general, the kinetic data available regarding copolymerization reactions at

elevated temperatures are limited. This may stem from the fact that extra complexities are encountered at elevated temperatures. These include the effects of reaction thermodynamics. Polymerizations are governed by standard free energy relationships and are generally exothermic.

$$\Delta G = \Delta H - T\Delta S \quad (1)$$

In ‘normal’ polymerization systems high values for  $\Delta H$  outweigh the entropy term, thus ensuring the negative  $\Delta G$  that is necessary for chain propagation. Hence, in the development of standard polymerization kinetic models, there is a general assumption that polymerization is not a reversible reaction. However, in systems where monomers have relatively low  $\Delta H$  values or at elevated temperatures, the value of  $\Delta G$  may no longer be negative, thus allowing for a predominance of the reverse reaction:



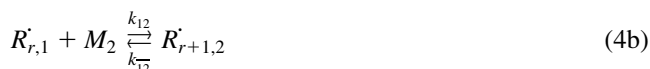
It can be shown that there is a temperature above which the reverse reaction is significant and formation of high polymer will be unfavorable:

$$\Delta G = -RT \ln K \quad (3)$$

This is termed the ceiling temperature. AMS has a relatively low ceiling temperature (61 °C for bulk monomer) [4], thus its homopolymerization is essentially impossible at the elevated temperatures examined in this work. Copolymerization with other monomers is therefore one method of producing AMS containing polymers at temperatures above 60 °C in a practical manner.

\* Corresponding author. Tel.: +1-519-888-4567; fax: +1-519-888-6179.  
E-mail address: penlidis@cape.uwaterloo.ca (A. Penlidis).

Kinetic models describing copolymerization of AMS have to take into account depropagation because of its unusually low ceiling temperature. Attempts to derive models, which account for depropagation in copolymerizations, have been made by Lowry [5], Wittmer [6] and Kruger et al. [7]. Consider the different possible reaction permutations when the four standard radical/monomer reaction pairings for a copolymerization are reversible:



Lowry's approach to solve for the kinetics of copolymerization with depropagation was an extension of the steady-state kinetic solution which leads to the Mayo–Lewis (M–L) equation. Lowry's model requires knowledge of the equilibrium constants for any reversible propagation reactions in addition to the normal reactivity ratios. In Lowry's case I, it is assumed that depropagation is significant only when monomer of type 2 ( $M_2$ ) is attached to radical of type 2 ( $R'_{r,2}$ ). In Lowry's case II, it is assumed that depropagation is significant only when  $M_2$  is attached to a sequence of two or more  $M_2$  units. This leads to more complex expressions. The model developed by Wittmer to account for instantaneous copolymer composition in a system where all possible reactions are reversible, is even more complex. All these models and their equations have recently been discussed in detail in Palmer et al. [8,9].

There is a continued interest in the copolymerization of AMS with various monomers. Most recently, Martinet et al. [10–12] investigated the copolymerization with MMA in solution, bulk and emulsion. Physical analyses of the copolymer products were made and models were proposed to account for the nature of these products. Another recent paper, by Pazhanisamy et al. [13] investigated the copolymerization of AMS with *N*-cyclohexylacrylamide. They utilized NMR data to characterize the copolymers and carried out reactivity ratio estimations. Christiansen [14] used data from Izu and O'Driscoll [15] to evaluate the model he developed concerning the moments of the chain distribution for low conversions, in a system with reversible propagation. The applicability of terminal model kinetics in the copolymerization of AMS with methacrylonitrile was also considered by Fleischauer et al. [16]. These authors used sequence length data from [13] C NMR spectra of copolymers with a range of compositions to attempt descri-

mination between the appropriateness of terminal and penultimate models.

Various groups have examined copolymerizations of AMS with a number of common monomers. For instance, O'Driscoll and Dickson [17] studied the copolymerization of styrene with AMS at 60 °C using Lowry's models. In a series of papers, Fischer [18,19] looked at the kinetics for various alpha-substituted styrenes with styrene. These studies included an investigation of copolymerizations over a range of temperatures (60–150 °C) using the Wittmer models. Estimations of the retardation effect caused by addition of the alpha-substituted monomers were also made. The data set on the styrene/AMS system was further developed by Rudin and coworkers [2,3,20] who looked at both solution and emulsion copolymerization. Branston et al. [21] also did some work on emulsion polymerization of styrene/AMS. They produced copolymers from a number of feed compositions and assessed the physical properties of the products. A study of styrene/AMS copolymerization was conducted by Barson and Fenn [22]. They showed that effects of depropagation in copolymerization could be ignored for reactivity ratio estimation when using feeds containing low levels of AMS.

Katsukiyo and Kodaira [23] estimated reactivity ratios and the equilibrium constant of AMS with MMA at 60 °C. A series of papers by O'Driscoll and coworkers [15,24–26] included detailed analyses of copolymer properties, including composition, coisotacticities, and chain length. Mechanistic derivations in this series of papers included a copolymer composition equation based on probability density functions, which had to be evaluated using Monte Carlo techniques. Wittmer also used the AMS/MMA as the experimental system to support his model derivation [5,27]. He examined the copolymerization over the range 60–150 °C and estimated various kinetic parameters from the model in conjunction with the data collected. Motoc and Vancea have also looked at this system and analyzed Wittmer's data using a Markov chain model [28].

The present study describes the first examination of the copolymerization of BA with AMS. The work is separated into two parts. In the first, low conversion studies were carried out at five temperatures in order to assess the applicability of different copolymerization models and obtain reactivity ratio estimates. In the second part, studies at two temperatures looked at rates, copolymer composition and molecular weight development over the full conversion range.

## 2. Experimental methods

### 2.1. Reagent purification

Monomers obtained from Aldrich Chemical Company were purified by washing three times with a 10% sodium hydroxide solution, followed by three washes with de-ionized

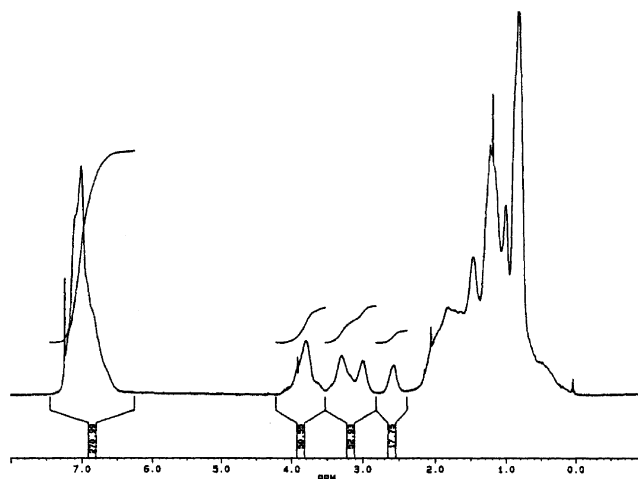


Fig. 1.  $^1\text{H}$  NMR spectrum of BA/AMS copolymer.

water [29]. The monomers were dried over calcium chloride and stored at  $-10\text{ }^\circ\text{C}$ . Immediately prior to reaction they were distilled under reduced pressure. 2,2'-azo-bisobutyronitrile (AIBN, Polysciences Inc.), was recrystallized three times from absolute methanol. Di-*t*-butyl peroxide (Trigonox-B (Trig-B), AKZO), dodecyl mercaptan (NDM) (Aldrich Chemicals) as chain transfer agent (CTA) and solvents (ethanol, acetone and chloroform-*d*), were used as received without further purification.

### 2.2. Low conversion experiments

Experiments were carried out in glass ampoules having a volume of ca. 5 ml. Stock solutions of the monomer and initiator (AIBN for 60 and  $80\text{ }^\circ\text{C}$ , Trig-B for all other temperatures) were prepared by weighing appropriate amounts of reagents and then ca. 2 ml aliquots were transferred by pipette into the ampoules. Degassing of the monomer solution was done by several vacuum-freeze-thaw cycles. The ampoules were then flame-sealed and stored in liquid nitrogen until ready for use. Reaction was carried out by placing the ampoules in a temperature-controlled bath for an appropriate time interval. Polymer products were obtained by rapid evaporation of volatiles to produce films. Drying of the samples was completed in a vacuum oven at  $70\text{ }^\circ\text{C}$ . Conversion was determined gravimetrically by comparison of polymer weights with weights of the feeds.

### 2.3. Full conversion range experiments

Experimental procedures were essentially the same as for the low conversion studies, except that in order to remove polymer from the ampoules at conversions above ca. 50% the ampoules were frozen and then cut into small sections. These sections were allowed to soak in acetone at room temperature until the contents fully dissolved. Following this the work up was as above.

## 3. Copolymer characterization

### 3.1. Copolymer composition: $^1\text{H}$ NMR spectroscopy

$^1\text{H}$  NMR spectra were recorded, using a Bruker AM 300 spectrometer, for samples of polymer dissolved in  $\text{CDCl}_3$ . Copolymer composition was calculated by comparison of the integrals from signals at ca. 4–2.5 ppm, assigned to the two protons of the  $-\text{OCH}_2-$  group of butyl acrylate (BA), and the broad signals at ca. 7 ppm, due to the aromatic protons (5H per mole) of AMS (see Fig. 1). It is believed that the wide range of chemical shifts, observed for the O- $\text{CH}_2$  signal, stems from different triad and tacticities possible for the copolymer, and similar assignments have been documented for AMS/MMA [25].

### 3.2. Molecular weights

Molecular weights were obtained using a Waters GPC system operating at  $25\text{ }^\circ\text{C}$ , with THF as the eluent. Samples were prepared as 0.5% solutions in THF. The system detectors were a multi-angle laser light scattering (MALLS) (Wyatt Dawn DSP-F) operating at 630 nm and a Waters DR401 differential refractive index detector (DRI). Wyatt Astra software was used for data analysis. The method used  $dn/dc$  values to calculate molecular weights and for the copolymers these were obtained by calculating averages based on  $dn/dc$  values for the homopolymers [30,31] and copolymer compositions.

## 4. Results and discussion

### 4.1. Low conversion studies

Estimation of reactivity ratios was carried out at five temperatures (60, 80, 100, 120 and  $140\text{ }^\circ\text{C}$ ) to ascertain how the system behaved with respect to the various copolymerization models as a function of temperature. Copolymer composition data from low conversion range polymerizations ( $<5\%$ ) were collected with respect to the different monomer feed compositions. In order to obtain sufficient data for reliable parameter estimation, several feeds were chosen along the range of possible monomer feed compositions with replicates being run at selected feeds.

Fig. 2a shows composition data (mole fraction AMS in copolymer vs mole fraction in the feed) for the copolymers obtained at 60 and  $140\text{ }^\circ\text{C}$ . The plot shows that as the reaction temperature increases the maximum achievable level of AMS in the copolymer drops to the limiting level of ca. 50%, which is observed at  $140\text{ }^\circ\text{C}$ . The data from the other temperatures (Fig. 2b) show that there is a steady consistent decrease in the maximum achievable level of AMS in the products as the reaction temperature increases (note, expanded y-scale used to distinguish trends at different temperatures).

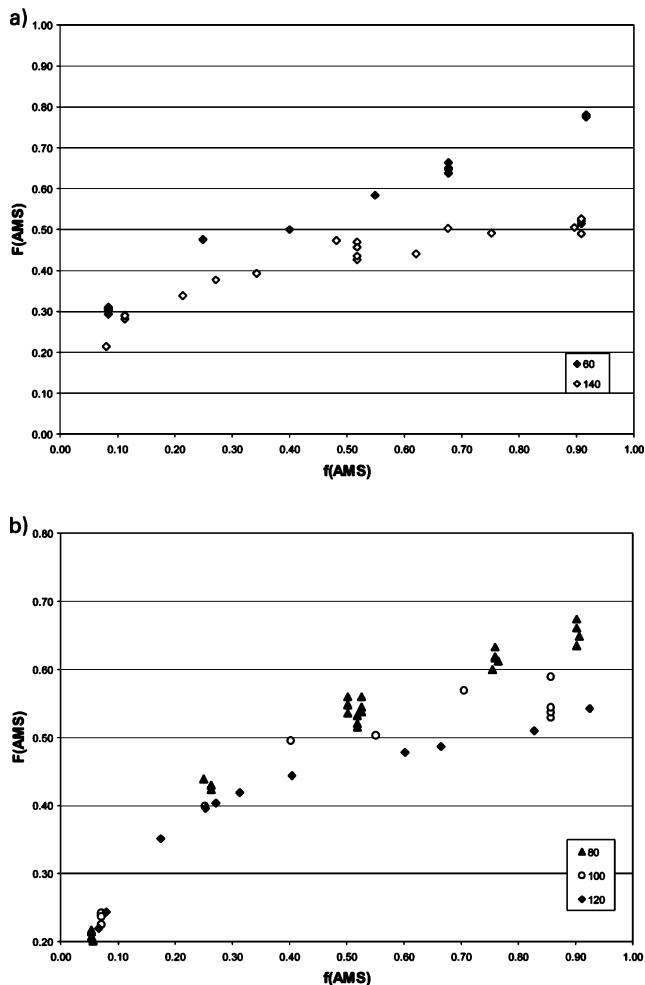


Fig. 2. Copolymer composition vs. monomer feed composition at different temperatures (a) 60 and 140 °C. (b) 80, 100 and 120 °C.

The data were analyzed with respect to different copolymerization models: the M–L model, Lowry models I and II (only homopolymerization of AMS reversible) and the simplified Wittmer model that assumed only the homopolymerization of AMS is reversible. For the M–L basic model, estimates of the ‘apparent’ reactivity ratios were obtained using the Error in Variables Model (EVM) method, utilizing raw NMR data in conjunction with monomer feed composition data [32]. For the Lowry and Wittmer expressions, data were analyzed by non-linear regression techniques. The values obtained for the reactivity ratios by the M–L and Lowry models are presented in Table 1. Results from all the models were similar. The Wittmer model is more prone to numerical instabilities as observed also with MMA/AMS [8,9].

Earlier studies attempting to interpret copolymerization systems that may be affected by monomer depropagation have used the Arrhenius expression ( $\ln(r)$  vs.  $1/T$ ) as a measure of whether a model adequately describes the copolymerization. The implication of a linear fit, over a range of temperatures, for the expression implies that the

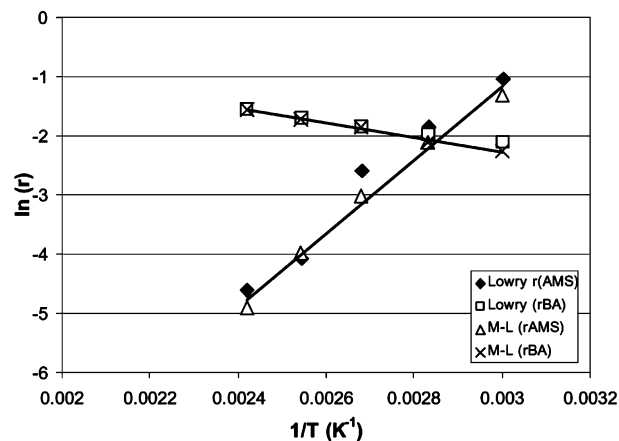


Fig. 3. Arrhenius plot for M–L and Lowry case II models, reactivity ratios.

model is appropriate with respect to predicting reliably copolymer composition [33]. Therefore, Arrhenius plots of  $\ln(r)$  vs.  $1/T$  were made for the observed reactivity ratio values for the M–L and Lowry (case II) models, and are shown in Fig. 3.

The plots show that the trends are essentially linear for both models. The temperature dependence of the reactivity ratios for the M–L model estimates can be expressed as:

$$\ln(r_{\text{BA}}) = 1.5064 - 1264/T \quad (5a)$$

$$\ln(r_{\text{AMS}}) = -19.8 + 6213/T. \quad (5b)$$

The temperature dependence for the Lowry case II estimates can be expressed as:

$$\ln(r_{\text{BA}}) = 0.736 - 955/T, \quad (6a)$$

$$\ln(r_{\text{AMS}}) = -20.9 + 6457/T. \quad (6b)$$

where  $T$  is in degrees K.

Our results indicate that, for low conversion polymerizations, even the M–L model in conjunction with apparent reactivity ratios will adequately describe trends in copolymer composition over a wide range of feed compositions and temperatures.

#### 4.2. Full conversion range studies

The principal objective of the full conversion range

Table 1  
Reactivity ratios for BA/AMS copolymerization at various temperatures

Temperature (°C)	Mayo–Lewis		Lowry I		Lowry II	
	$r_{\text{BA}}$	$r_{\text{AMS}}$	$r_{\text{BA}}$	$r_{\text{AMS}}$	$r_{\text{BA}}$	$r_{\text{AMS}}$
60	0.118	0.298	0.119	0.354	0.120	0.354
80	0.149	0.153	0.142	0.157	0.139	0.157
100	0.168	0.052	0.165	0.051	0.157	0.075
120	0.166	0.022	0.181	0.017	0.181	0.017
140	0.191	0.009	0.208	0.010	0.210	0.010

Table 2  
Copolymerization of BA/AMS. Experimental details for full conversion runs

Run #	Temperature (°C)	BA/AMS ratio <sup>a</sup>	[Trig B] <sup>b</sup>	[CTA] <sup>b</sup>
1	115	55/45	1.5	0.2
2	115	55/45	3.0	0.2
3	140	55/45	0.4	0.2
4	140	55/45	1	0.2
5	140	55/45	1.6	0.2
6	115	55/45	1.5	0.41
7	140	40/60	1.6	0.2

<sup>a</sup> Weight ratio.

<sup>b</sup> Weight percent.

studies was to examine kinetic behavior of the system and collect a body of data for the system with respect to feed composition, initiator concentration and reaction temperature. Given that the reactivity ratio studies had shown that the effects of AMS depropagation were limited, it was of interest to see if this was also true for full conversion range polymerizations.

Two temperatures were studied (115 and 140 °C). At each temperature level various initiator concentrations were used. The primary feed chosen for study had a BA/AMS ratio of 55/45 (by weight). This represents a feed that would be close to the limit for complete AMS incorporation in the polymer over the whole conversion range (i.e. 50 mol%). The second feed was chosen to observe the system behavior with what would be an excess of AMS, if one assumes that the maximum incorporation of AMS would be ca. 50%, at the chosen reaction temperatures. Table 2 summarizes the details of the copolymerizations carried out. All runs were carried out with added CTA in order to avoid gel formation that is encountered when studying polymerizations involving BA [1].

Figs. 4 and 5 show the conversion vs. time plots for reactions at 115 and 140 °C, respectively, with feeds having a BA/AMS ratio of 55/45. The reactions at 115 °C proceed to approximately 100% conversion of monomers. Fig. 4

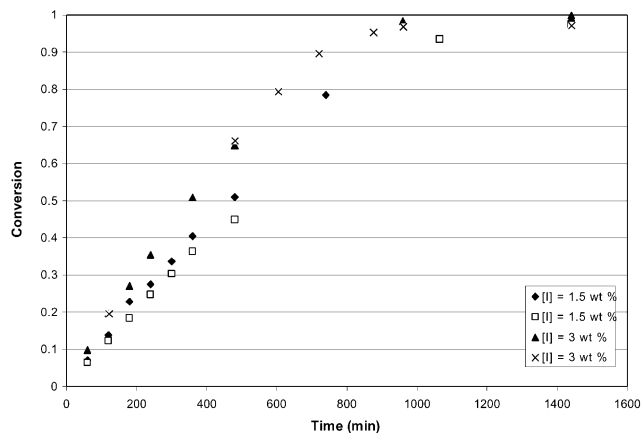


Fig. 4. Conversion vs. time.  $T = 115$  °C, BA/AMS = 55/45, [CTA] = 0.2%. Effect of [I].

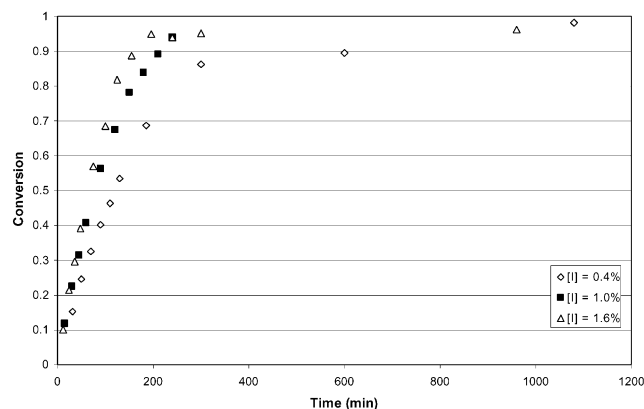


Fig. 5. Conversion vs. time.  $T = 140$  °C. BA/AMS = 55/45, [CTA] = 0.2%. Effect of [I].

shows data from two runs at each condition. This was done to check experimental reproducibility and to obtain complimentary points for the original data sets. The auto-acceleration phase typically seen for full conversion polymerizations in bulk is not very pronounced but possibly manifests itself by producing an apparent zero order dependence on monomer concentration for conversions up to ca. 90%. The increase in rates, observed in going from 1.5 to 3.0% initiator, is a factor of ca. 1.3, which is about that expected for the normal square root dependence on initiator concentration.

The reactions at 140 °C typically tail off at 96–98%. This presumably is a vestige of the effect of AMS depropagation. At these temperatures, AMS can only incorporate in the polymer via copolymerization, thus when the concentration of BA in the polymerizing mixture approaches zero, the polymerization rate will slow down considerably. The rate increase with changes in [I] is slightly less than expected based on the standard square root dependence with [I]. The reason for this probably is a result of thermal initiation of monomer, which is likely for AMS. Impurities in monomers (BA) are also known to act as initiators at elevated

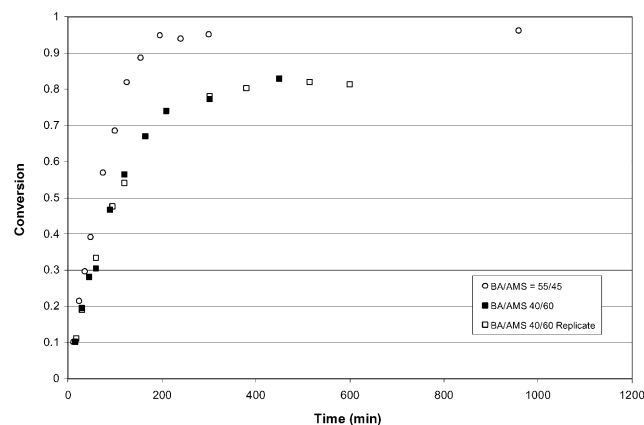


Fig. 6. Conversion vs. time,  $T = 140$  °C. [CTA] = 0.2%, [I] = 1.6%. Effect of monomer ratio.

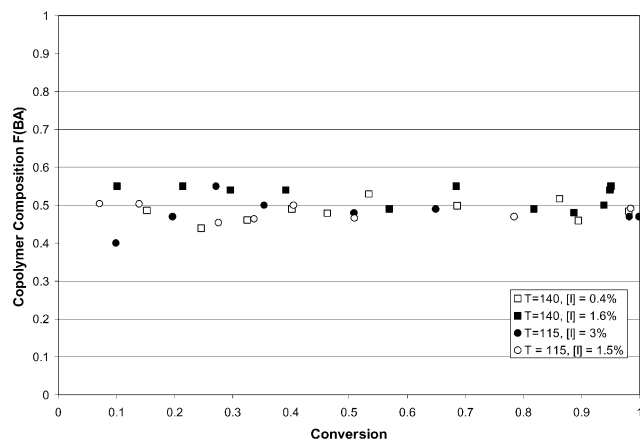


Fig. 7. Copolymer composition. BA/AMS = 55/45. Effect of temperature and [I].

temperatures as has been shown in the thermal polymerization of MMA [34] and observed with BA in our group. An initiation effect from trace impurities in the monomers is therefore likely.

Increasing the level of AMS in the feed has a marked effect on the conversion rate profile. Fig. 6 shows conversion vs time for two runs, at 140 °C, where the only difference is the monomer ratio. It is apparent that increasing the amount of AMS leads to a significant reduction in the rate of reaction. In addition, complete conversion of the monomers was not observed. The reaction reaches an equilibrium conversion level of ca. 80%. Assessment of copolymer composition at the equilibrium monomer conversion levels shows that at ca. 80% conversion, the BA monomer concentration in the feed is approaching zero. Thus the residual unreacted monomer is approximately 100% AMS and further polymerization is not possible because AMS will not homopolymerize under the chosen reaction conditions.

Fig. 7 shows the trends in cumulative copolymer composition with conversion of monomer for BA/AMS feeds with a monomer ratio of 55/45. The apparent lack of drift in composition with conversion of monomer is striking.

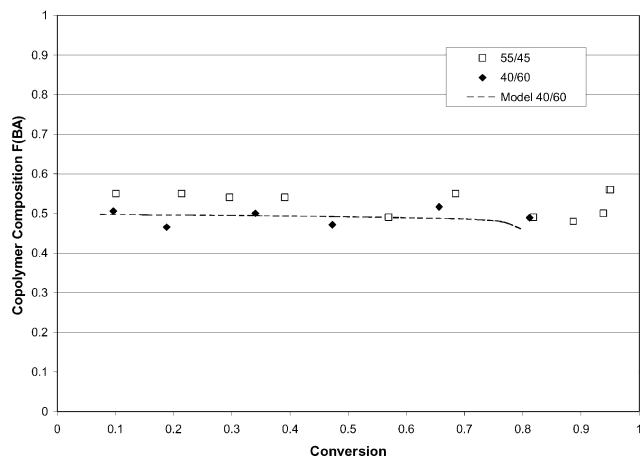


Fig. 8. Copolymer composition. Effect of BA/AMS feed ratio.

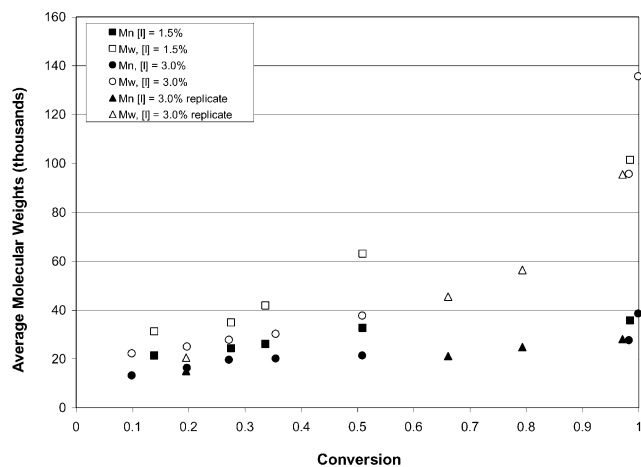


Fig. 9. Trends in average molecular weights,  $T = 115$  °C, BA/AMS = 55/45, [CTA] = 0.2%. Effect of [I].

Fig. 8 shows the copolymer composition observed for feeds containing the higher level of AMS. An increase of 33% in the feed leads to only a slightly higher incorporation of AMS in the copolymer (ca. 2%). As was observed for polymerizations, which used the (55/45) monomer feed ratio, the cumulative copolymer composition is largely independent of the degree of monomer conversion. This ‘pseudo-azeotropic’ behavior was also noted in the copolymerization of AMS with MMA and was related to having two monomers that could depropagate under the chosen reaction conditions [8]. In the case presented here, the standard Meyer–Lowry (integrated) model (see model line in Fig. 8) based on apparent reactivity ratios derived using the M–L relationship can account for the lack of composition drift without bringing in factors related to depropagation.

Figs. 9 and 10 show the trends observed for molecular weight averages at 115 and 140 °C, respectively, for reactions where the BA/AMS ratio was 55/45. In the figures it can be seen that, for both temperatures, the observed

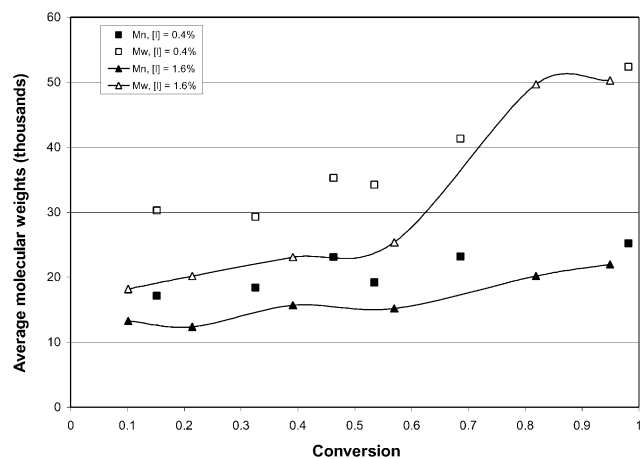


Fig. 10. Trends in average molecular weights,  $T = 140$  °C, BA/AMS = 55/45, [CTA] = 0.2%. effect of [I].

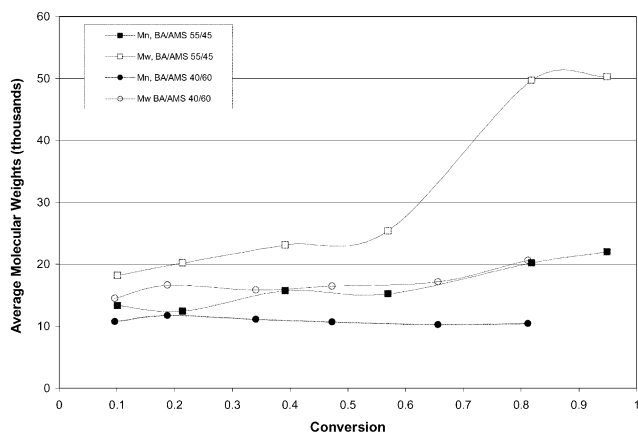


Fig. 11. Trends in average molecular weights.  $T = 140\text{ }^{\circ}\text{C}$ ,  $[\text{I}] = 1.5\%$ ,  $[\text{CTA}] = 0.2\%$ . Effect of monomer feed ratio.

molecular weight averages are lower for feeds that have higher initiator concentrations, as expected.

Fig. 11 shows the trends in molecular weight observed in the experiment where the initial proportion of AMS in the feed is 60%. The molecular weights are lower for the feed higher in AMS. In addition, the molecular weights are relatively consistent across the complete range of conversion. In contrast to experiments where the ratios of monomers are almost equal, there is no increase in  $M_w$  as the reaction reaches its limiting conversion level. This probably is because there is always an excess of AMS monomer in the reaction, which acts as a virtual chain transfer agent controlling (lowering) the molecular weight.

Fig. 12 shows the conversion rates for two feeds where the only difference is the level of CTA (NDM = *n*-dodecylmercaptan). It can be seen that, for the conditions chosen, doubling the level of CTA has essentially no effect on the reaction rate. This is an indicator that there is a minimal 'gel effect' for the system, because higher levels of CTA normally lead to a suppression of auto-acceleration caused by the gel effect. Fig. 13 shows the molecular weight

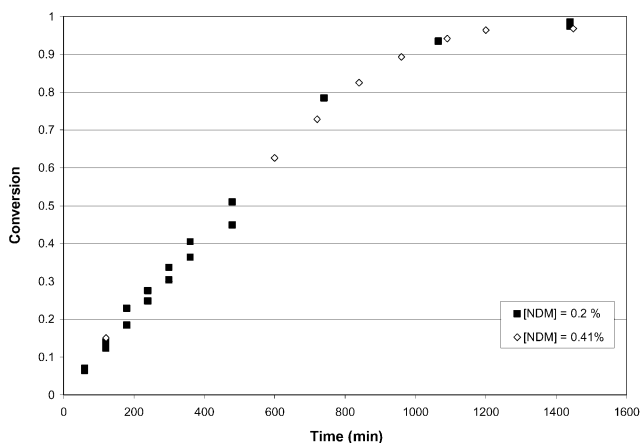


Fig. 12. Conversion vs. time.  $T = 115\text{ }^{\circ}\text{C}$ ,  $[\text{I}] = 1.6\%$ . Effect of  $[\text{CTA}]$ .

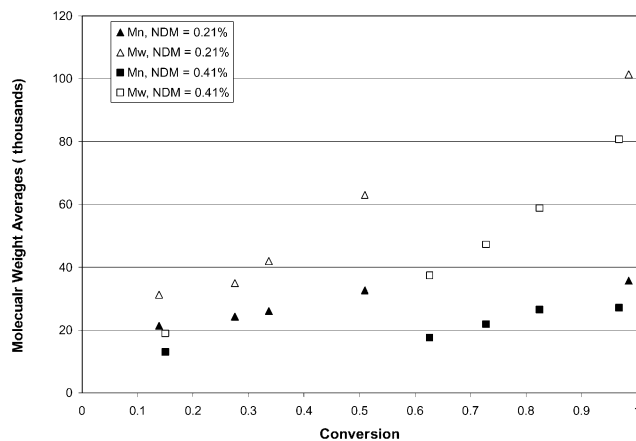


Fig. 13. Trends in average molecular weight.  $T = 115\text{ }^{\circ}\text{C}$ .  $[\text{I}] = 1.6\%$ . Effect of  $[\text{CTA}]$ .

averages for these experiments and the expected drop in molecular weights with increasing CTA concentration.

Glass transition temperatures were measured for selected samples from two of the experiments; runs 1 and 3. The results are presented in Table 3. The  $T_g$  values obtained for samples produced at  $115\text{ }^{\circ}\text{C}$  were slightly higher than for the  $140\text{ }^{\circ}\text{C}$  run, as expected.

## 5. Conclusions

This is the first study examining the copolymerization of BA with AMS. Low conversion copolymerizations have been carried out over a range of temperatures and reactivity ratios have been assessed from these data with respect to different polymerization models. The trends in reactivity ratios with temperature follow the Arrhenius relationship indicating that the models describe the system adequately with respect to composition of copolymer, for low conversion polymerization. Full conversion data also have been collected. Rates, copolymer composition and molecular weight development with respect to monomer ratio, initiator concentration and CTA concentration were examined. It has been found that, for the chosen feeds, the M–L model describes cumulative composition well with respect to monomer conversion. The data collected show also that

Table 3  
Glass transition temperatures for selected BA/AMS copolymer products

Reaction details	Conversion (%)	Composition F(AMS)	$T_g$ ( $^{\circ}\text{C}$ )
$T = 115\text{ }^{\circ}\text{C}$	13.9	0.496	26
$[\text{I}] = 1.48\%$	40.5	0.500	26
$[\text{NDM}] = 0.2\%$	78.4	0.530	30
$T = 140\text{ }^{\circ}\text{C}$	15.2	0.514	19
$[\text{I}] = 0.4\%$	32.5	0.539	23
$[\text{NDM}] = 0.2\%$	46.3	0.521	25
	98.2	0.516	25

increasing the AMS level above ca. 50% will not lead to complete conversion of monomers and so monomer/polymer equilibrium effects are significant.

### Acknowledgements

We gratefully acknowledge: the Natural Sciences and Engineering Research Council (NSERC) of Canada and ICI, Worldwide for funding; Dean Palmer and Tina Wang (graduate students); Simone Buckley, Shahaveer Jamshedji (undergraduate research assistants) and Vincent Verhoeven (exchange student from the Netherlands) for experimental help. Many thanks to Professor Morris Tchir (Chemistry, Waterloo) for his help in NMR analysis.

### References

- [1] Gao J, Penlidis AJ. *Macromol Sci-Macromol Rev* 1998;38:651–780.
- [2] Rudin A, Chiang SSM. *J Polym Sci* 1974;12:2235–54.
- [3] Rudin A, Samanta MC. *J Appl Polym Sci* 1979;24:1665–89.
- [4] McKormick HW. *J Polym Sci* 1957;25:488.
- [5] Lowry GG. *J Polym Sci* 1960;42:463–77.
- [6] Wittmer P. *Adv In Chem Ser* 1971;99:140–74.
- [7] Kruger HJ, Bauer J, Rubner J. *J Makromol Chem* 1987;188:2163–75.
- [8] Palmer DE, McManus NT, Penlidis A. *J Polym Sci A Chem Ed* 2000;38:1981–90.
- [9] Palmer DE, McManus NT, Penlidis A. *J Polym Sci A Chem Ed* 2001;39:1753–63.
- [10] Martinet F, Guillot J. *J Appl Polym Sci* 1997;65:2297–313.
- [11] Martinet F, Guillot J. *J Appl Polym Sci* 1999;72:1611–25.
- [12] Martinet F, Guillot J. *J Appl Polym Sci* 1999;72:1627–43.
- [13] Pazhanisamy P, Ariff M, Anwaruddin Q. *J Macromol Sci, Pure Appl Chem* 1997;A34:1045–54.
- [14] Christiansen RL. PhD Thesis. University of Wisconsin, 1990.
- [15] Izu M, O'Driscoll KF. *J Polym Sci: Part A-1* 1970;8:1687–91.
- [16] Fleischauer J, Schmidt-Naake G, Scheller D. *Die Angew Makromol Chem* 1996;243:1–37.
- [17] O'Driscoll KF, Dickson JR. *J Macromol Sci-Chem* 1968;A2:449–57.
- [18] Fischer JP. *Die Makromol Chem* 1972;155:211–25.
- [19] Fischer JP. *Die Makromol Chem* 1972;155:238–57.
- [20] Rudin A, Samanta MC, Van der Hoff BMEJ. *Polym Sci Chem Edn* 1979;17:493–502.
- [21] Branston RE, Plaumann HP, Sendorek JJ. *J Appl Polym Sci* 1990;40:1149–62.
- [22] Barson CA, Fenn DR. *Eur Polym J* 1986;22:195–7.
- [23] Katsukiyo I, Kodaira K. *Polym J* 1986;18:667–72.
- [24] O'Driscoll KF, Gasparro FP. *J Macromol Sci Chem Edn* 1967;A1:643–52.
- [25] Howell JA, Izu M, O'Driscoll KF. *J Polym Sci: Part A-1* 1970;8:699.
- [26] Izu M, O'Driscoll KF, Hill RJ, Quinn MJ, Harwood HJ. *Macromolecules* 1972;5:90–92.
- [27] Wittmer P. *Die Makromol Chem* 1967;103:188–213.
- [28] Motoc I, Vancea R. *J Polym Sci, Polym Chem* 1980;18:1559–64.
- [29] Stickler M. *Macromol Symp* 1987;10/11:17–69.
- [30] McManus NT, Penlidis A. *J Appl Polym Sci Polym Chem* 1998;70:1253–4.
- [31] Brandrup J, Immergut EH. *Polymer handbook*. New York: Wiley Interscience, 1989.
- [32] Polic L, Duever TA, Penlidis A. *J Appl Polym Sci Polym Chem* 1998;36:813–22.
- [33] Ueda M, Suzuki T, Takahashi M, Li ZB, Koyama K, Pittman Jr. *CU. Macromolecules* 1986;19:558–65.
- [34] Clouet G, Chaumont P, Corpart P. *J Polym Sci Chem Edn* 1993;31:2815–24.